Study on Microstructures and Resist Corrosion Properties of Two-Step Hot-Dipping Al - Zn Composite Coating on Q345 Steel

Chong Tian and Faguo Li *

Posted Date: 7 August 2023

doi: 10.20944/preprints202308.0484.v1

Keywords: Q345 steel; Two-step Hot-dipping method; Al - Zn composite coatings; microstructures; resist corrosion properties

Article

Study on Microstructures and Resist Corrosion Properties of Two-Step Hot-Dipping Al - Zn Composite Coating on Q345 Steel

Chong Tian and Faguo Li *

School of Materials Science and Engineering, Xiangtan University, Xiangtan 411105, China; T1430777965@163.com (C.T.)

* Correspondence: lifaguo@xtu.edu.cn (F.L.)

Abstract: Q345 steel is widely used in the construction industry, vehicle manufacturing industry, bridge construction industry and many other aspects due to its excellent comprehensive performance. However, due to its high silicon content, direct hot-dip galvanizing will lead to a series of problems, such as easy peeling of the coating due to the "silicon reactivity". In this paper, we adopt the "two-step hot-dipping method", first hot-dip aluminizing and then hot-dip galvanizing, to isolate the substrate and zinc liquid direct contact, so as to avoid the occurrence of "silicon reactivity". Through the microstructure characterization, neutral salt spray corrosion experiments, electrochemical experiments, the results show that: Al-Zn composite coatings from the inside out were perpendicular to the substrate growth of loose Fe_2Al_5 layer and Al-Zn layer, outbursts generation; Al-Zn composite coatings resistance to neutral salt spray corrosion was far more than the substrate; Al-Zn composite coatings polarization curve corrosion potential than the substrate was lower than that of the substrate by 0.512V, showing a strong corrosion resistance. It shows extremely strong corrosion resistance.

Keywords: Q345 steel; two-step hot-dipping method; Al - Zn composite coatings; microstructures; resist corrosion properties

1. Introduction

Q345 steel is a commonly used structural steel with a wide range of applications, and its main components include carbon (C), silicon (Si), manganese (Mn), phosphorus (P), sulfur (S) and other elements. Its carbon content is usually between 0.12 wt.% and 0.20 wt.%. Carbon is one of the main alloying elements of Q345 steel, and it increases the hardness and strength of the steel. A moderate carbon content increases the hardness and wear resistance of Q345 steel while maintaining good workability. And its silicon content usually ranges from 0.20 wt.% to 0.55 wt.% [1]. Silicon acts as a deoxidizer and enhancer of grain boundaries in steel, which can improve the strength and corrosion resistance of steel. A moderate amount of silicon helps to improve the weldability and corrosion resistance of Q345 steel. In terms of performance, it is characterized by high strength, good corrosion resistance, weldability, good plasticity and toughness, and low temperature influence. In terms of strength, Q345 steel has high yield strength and tensile strength. Depending on the state of the material, its yield strength is usually between 345MPa and 470MPa, and its tensile strength is between 470MPa and 630MPa. This enables Q345 steel to withstand large loads and pressures in structural engineering [1]. In terms of corrosion resistance, Q345 steel has good corrosion resistance and can be used for a long time in harsh environments such as wet and rainy conditions without easy rusting or corrosion. This makes Q345 steel widely used in marine engineering, chemical equipment and other fields. Similarly, in terms of weldability, its good weldability enables it to be connected and processed by common welding methods. This gives Q345 steel an advantage in structural assembly, welded fabrication and so on. In conclusion, Q345 steel, as a commonly used structural steel, is characterized by stable composition, high strength, good corrosion resistance, strong weldability, good plasticity and toughness. These properties make Q345 steel widely used in construction, bridges, ships, petrochemical equipment and other fields. However, with its own performance is difficult to use

 doi:10.20944/preprints202308.0484.v1

directly in a variety of projects, so people often surface treatment to strengthen its performance, commonly used methods are electroplating, painting, hot-dip galvanizing and so on. Hot-dip galvanizing and hot-dip aluminizing are the common treatment methods for Q345 steel.

Hot-dip galvanizing is a corrosion protection method in which steel is immersed in molten liquid zinc to form a protective alloy layer on its surface. The advantage of zinc is that it can form a dense protective coating on the surface of the steel to isolate it from the air, and it can be sacrificed to protect the substrate with an anode [2]. Since zinc corrodes at a much lower rate than steel, it can effectively protect steel and greatly improve its corrosion resistance, giving it a service life of decades [3,4]. With the progress of technology, the galvanizing technology becomes more and more advanced, it has the characteristics of easy operation, wide coverage, strong corrosion resistance, close connection with the substrate, high durability, and low maintenance cost, thus, the steel products treated by hot-dip galvanizing technology have been applied to various industries, such as infrastructure, electric power, transportation, construction, communication, energy, etc., which has an increasingly wide range of applications, and has an extremely high development potential[5–7]. Despite the fact that hot-dip galvanizing is a long-established and mature process, there are still many technical problems with galvanizing steel containing silicon. Silicon in steel is either present as a residue of the deoxidizer in the smelting process or as a strengthening element. In general galvanizing, silicon in steel causes the surface of the coating to appear dark gray, the coating to be too thick, and the bonding strength between the coating and the substrate to be reduced, a phenomenon known in industry as "silicon reactivity" [8](also known as the Sandelin Effect). This problem has long plagued the galvanizing industry, especially affecting the development of the hot-dip galvanizing industry for high-strength structural steel. In order to solve these problems, people have tried to take many measures, for the higher silicon content of Q345 steel, can be pretreated to reduce the silicon content and reactivity. Common pretreatment methods include pickling and sanding, which remove oxidized layers and impurities from the steel surface, thus reducing the presence of silicon. During hot-dip galvanizing, a suitable galvanizing process can be selected to reduce silicon reactivity. For example, the Continuous Galvanizing Process (CGP) can be used to gradually increase the temperature in a series of dipping baths to better react the silicon with the zinc without precipitating it[9]. Similarly, in hot-dip galvanizing, reasonable process parameter settings can reduce the effect of silicon on the coating. For example, controlling parameters such as galvanizing temperature, dipping time and dipping speed make the galvanizing reaction more uniform and reduce the possibility of silicon precipitation.

In contrast, the process of hot-dip aluminizing of steel is carried out by adding elemental aluminum to the steel smelting process so that it reacts with the oxygen in the steel to form alumina (Al_2O_3)[10,11]. This reaction is highly exothermic and provides enough heat to maintain the temperature required during the smelting process. At the same time, alumina can react with other impurity elements (e.g., sulfur, oxygen, nitrogen, etc.) to reduce the amount of impurities in the steel. Aluminum solution containing a small amount of silicon is more capable of reducing the intermetallic compound layer[12–15]. Therefore, the steel hot-dip aluminizing achieves the dual role of heat supply and deoxidation and deimpurity. Hot-dip aluminizing can form a dense, uniform aluminum layer, effectively preventing the corrosion of steel. Aluminum has good corrosion resistance, can be under the protection of the oxide layer to prevent the steel and the outside world, such as oxygen, water and other substances in contact, and provides a long-term corrosion protection. It also provides some protection against heat. This makes Q345 steel hot-dip aluminizing has good high temperature resistance, suitable for high temperature working environment, such as furnaces, boilers and other equipment. And then the appropriate heat treatment can obtain better high temperature oxidation resistance [16–22]. At the same time, the hot-dip aluminizing Q345 steel has good electromagnetic shielding properties, which can effectively absorb and shield electromagnetic waves. This makes the steel of hot-dip aluminizing has a wide range of applications in the field of electronic communication, electromagnetic interference control, such as electronic equipment shells, electromagnetic shielding cover, etc. Q345 steel hot-dip aluminizing has excellent corrosion resistance, high temperature resistance, electromagnetic shielding performance and decorative properties. It has been widely used

 doi:10.20944/preprints202308.0484.v1

in several fields, improving the quality and durability of Q345 steel and meeting various specific needs. However, its complex process leads to high cost. At the same time, the plating, being softer, is easily damaged by external forces such as scratches, impacts and friction. Once the plating is broken, the steel surface is exposed, which can lead to corrosion and other problems. Moreover, the thickness of the aluminum layer in hot-dip aluminizing is usually thin, typically between tens and hundreds of microns. Compared to other surface treatments, such as hot-dip galvanizing, hot-dip aluminizing has a thinner coating thickness, so the corrosion protection it provides may be relatively low.

The "two-step hot-dipping method" is a method of hot-dipping one alloy layer on the surface of steel substrate and then hot-dipping another alloy layer, which can realize the metallurgical composite of the two alloy layers, and its pretreatment process is simple and easy to carry out, and it can effectively control the organization, morphology and thickness of the composite coating. Therefore, it has been widely used on galvanized aluminum alloy steel wires [23]. K.Tachibana [24] and others used "double plating method" to hot dip Zn-7Al alloy on the surface of steel parts, and the atmospheric corrosion experiments for 10 years showed that the corrosion resistance of double plated Zn-7Al alloy coating is 4 times higher than that of zinc coating.

For the "double plating method", the Al content is critical to the performance of zinc-aluminum coatings, and excellent corrosion, temperature, and aging resistance as well as bright appearance can be achieved by adjusting the Al content [25,26] . The application of zinc-aluminum alloys with double Galfan (Zn-5Al-0.1Re) coatings (Al mass fraction more than 10 wt.%) in the "double plating method" has received a lot of attention, but there is still a lack of coatings with a lower Al content. Studies of the "dual plating method" have shown that a change in Al content significantly alters the surface characteristics of zinc-aluminum alloys and thus their corrosion characteristics, providing more possibilities for the application of the "dual plating method" [27,28]. The two-step hot-dipping method is different from other coating production in that it can be realized by hot-dipping regardless of the complexity of the shape, and the equipment is simple, low-cost and easy to operate [29–31]. This study focuses on the tissue morphology, corrosion resistance of two-step hot-dipping plated Al-Zn composite coating on Q345 steel. The method of hot-dip aluminizing and then hot-dip galvanizing is adopted to avoid the "silicon reactivity" caused by the direct contact between zinc liquid and steel.

2. Experimental

2.1. Experimental materials

The experimental materials were mainly zinc ingot (99.99 wt.% Zn), aluminum ingot (99.99 wt.% Al) and Q345 steel plate of 20mm x 10mm x 3mm (Shandong Chengjian Iron & Steel Company Limited, Liaocheng, Shandong, China). A hole of 2mm diameter was drilled at one end of the steel plate and a wire was threaded through it to make a hot dipping specimen.

2.2. Experimental process

2.2.1. Pre-processing

First, the Q345 hot-dipping specimens were immersed in 80°C 10% NaOH + 5% Na_2CO_3 alkaline wash solution for 5~10min, followed by cleaning with water. Next, the specimen was put into 20% hydrochloric acid +0.5% hexamethylenetetramine acid wash solution for 3~4min ultrasonic cleaning, and then cleaned with water, and then put into the drying oven for drying (120°C).

2.2.2. Hot dip plating

Firstly, the dried Q345 hot-dipping specimen was immersed into the aluminum solution at 750°C for 1-10 min, then quickly removed and put into the zinc solution at 750°C for the second hot-dipping for 1-10 min. Finally, the Q345 hot-dipping specimen was removed and put into the air for natural cooling, then two-step hot-dipping of Al-Zn composite coatings can be obtained.

The prepared samples of two-step hot-dipping Al-Zn composite coatings were labeled as 1min+1min, 2min+2min, 4min+4min, 6min+6min, and 10min+10min according to the difference in

dipping time in Al and Zn liquids, respectively. Five specimens of each type were prepared to evaluate the stability of the process and to statistically measure the thickness of the alloy layer of the plated layer as a function of time. The relationship between the changes in the thickness of the alloy layer with time was evaluated. For the 2min+2min specimen with superior plating, 50 specimens were prepared for later neutral salt spray corrosion experiments and electrochemical experiments to evaluate the corrosion resistance of two-step hot-dipping Al-Zn composite coatings.

2.3. Microstructure and corrosion resistance test

2.3.1. Microstructure characterization methods

Detailed characterization of the surface microstructure of the coatings was carried out using SEM (ZEISS EVO MA10, Zeiss, Jena, Germany) and the phase composition was analyzed using EDS (OXFORD X-MAXN, Zeiss, Jena, Germany). Physical phase analysis of the surface corrosion products was carried out using an X-ray diffractometer (XRD, Ultima IV, Rigaku Co, Tokyo, Japan).

2.3.2. Corrosion resistance

Neutral salt spray corrosion experiments were performed on 2min+2min samples. The samples were subjected to neutral salt spray (NSS) determination using a salt spray water jet test bench (MIT-60A, Ningbo Jinhe Instrumentation Machinery Equipment Company, Ningbo, Zhejiang Province, China). A corrosion solution of 5% NaCl (pH=6.5~7.2) was used for the experimental procedure, and the temperature inside the laboratory chamber was controlled at (35±1)°C to ensure that the sedimentation rate reached 1~2mL/h per 80cm² of the measurement area.

Before the test, the sides and back of the plating were sealed with silicone rubber and left under natural conditions for 24 h. After the silicone gel was completely solidified, the specimen was weighed and recorded as m_1 . Then the NSS test was carried out at intervals of 40h, 120h, 160h, 200h, 240h, 280h, 320h, and 360h, respectively. Then the corrosion products on the surface of the specimen were removed and weighed as m_2 , and the corrosion rate v was calculated according to the following formula [unit: g/(m² ·h)].

$$v = \frac{m_1 - m_2}{At} \times 100\% \quad (1)$$

Where A is the surface area of the specimen (unit: m²) and t is the test time (unit: h).

An electrochemical workstation (Shanghai Chenhua Instrument Company CHI660E, Shanghai, China) was used to test the Tafel curve of the specimens. A 3.5% NaCl solution was used, a platinum electrode was used as an auxiliary electrode and a saturated calomel electrode (SCE) was used as a reference electrode. The specimen was closed with silica gel (leaving a working area of 1 cm²) and the scanning voltage was -1.5 to -0.2 V with a scanning rate of 2 mV/s.

3. Results and discussion

3.1. Microstructure of the coating

Figure 1 shown the microstructure of Al-Zn coatings with different hot-dipping times at 750°C. The hot-dipping coating had obvious layering phenomenon, which can be divided into two regions: the alloy layer immediately adjacent to the substrate (composed of Fe, Al, Zn) and the surface layer (dominated by Zn and Al-Zn) formed by the condensation of the dip plating liquid. As can be seen from Table 1, the bulk phase was Fe_2Al_5, and the outermost layer is the Al-Zn alloy layer. The loose Fe_2Al_5 phase grows perpendicular to the matrix. Figures 1(a)-(b) shown that the Fe_2Al_5 phase layer can be divided into a large and dense Fe_2Al_5 phase layer and a small and loose Fe_2Al_5 phase layer under the condition of short hot-dipping time. With the increase of the hot-dipping time, the Fe_2Al_5 phase layer shown only small and dense Fe_2Al_5 phase layer (Figure 1(c)-(e)).

Preprints (www.preprints.org) | NOT PEER-REVIEWED | Posted: 7 August 2023 doi:10.20944/preprints202308.0484.v1

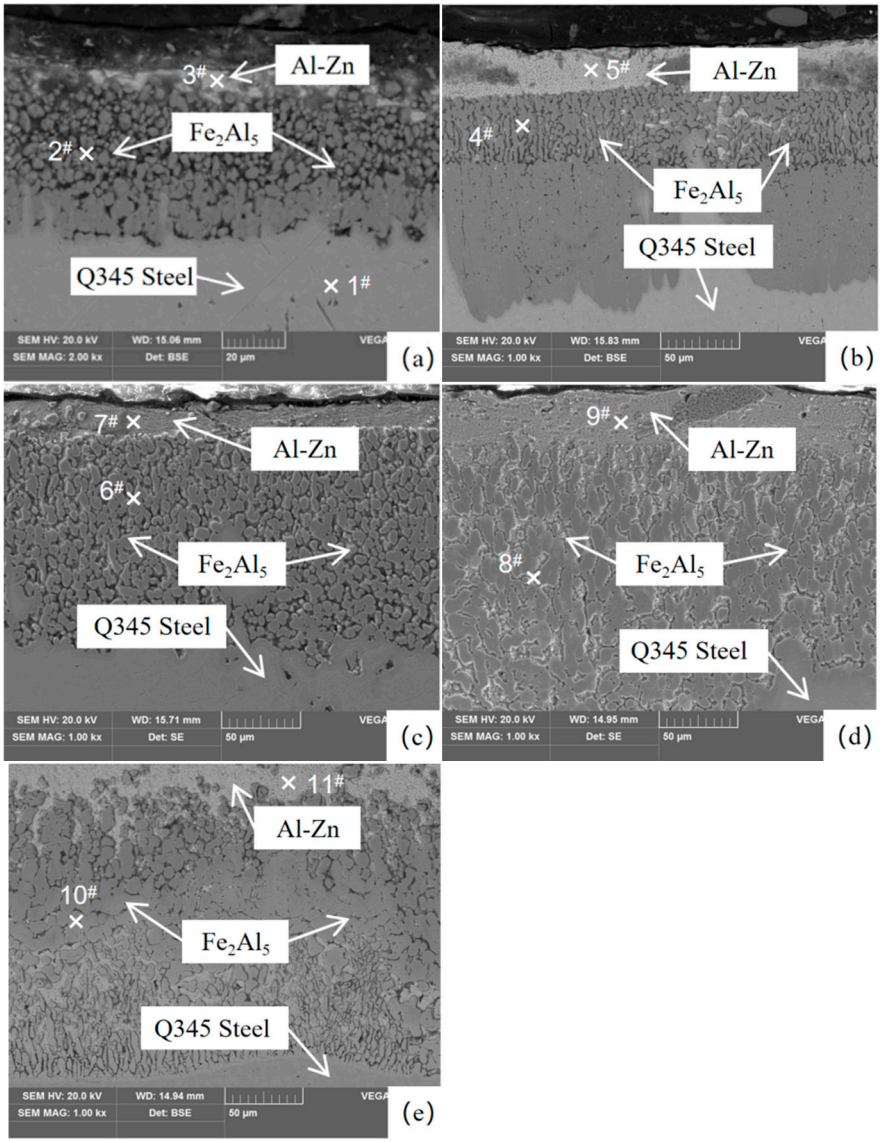

Figure 1. SEM images of Al-Zn composite coatings with two-step hot-dipping of Q345 at 750°C for (a) 1min+1min, (b) 2min+2min, (c) 4min+4min, (d) 6min+6min, (e) 10min+10min.

Table 1. EDS data (at.%) and phase compositions for the scan-point in Figure 1.

Analysis Region	Al	Fe	Zn	Phase
1#	0	99.99	0	Fe
2#	64.28	27.43	8.28	Fe_2Al_5
3#	22.60	66.57	10.83	Al-Zn
4#	64.87	26.52	8.60	Fe_2Al_5
5#	23.28	65.60	11.12	Al-Zn
6#	64.35	26.78	8.87	Fe_2Al_5
7#	21.75	65.89	12.36	Al-Zn
8#	64.42	27.26	8.32	Fe_2Al_5
9#	21.70	63.71	14.59	Al-Zn
10#	64.74	26.85	8.41	Fe_2Al_5
11#	22.34	63.52	14.14	Al-Zn

The relationship between the thickness of the alloy layer of Al-Zn composite coatings and time is usually expressed by us using the following empirical equation [32]:

Preprints (www.preprints.org) | NOT PEER-REVIEWED | Posted: 7 August 2023 doi:10.20944/preprints202308.0484.v1

$$\delta = Kt^n \quad (2)$$

where, δ is the thickness of the alloy layer (μm), t is the total time of the two-step hot-dipping (min), K is the rate constant, n is the kinetic index, and the kinetic index $n \leq 0.5$ is the diffusion-controlled growth, while $n > 0.5$ is the interfacial controlled growth (reaction-controlled growth).

In Figure 2, the fitting equation with n close to 0.5 indicates that the growth of Fe_2Al_5 alloy layer was controlled by diffusion through hot-dipping. From the fitted curves, it can be seen that the overall alloy layer thickness tends to increase with the increase of the hot-dipping time. The slope of the fitted curve decreased slightly as the hot-dipping time was greater than 8 minutes, resulting in a slowing down trend in the thickness growth.

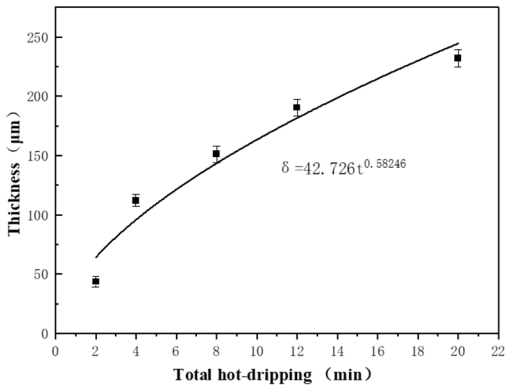

Figure 2. The thickness curve of Al-Zn composite coating's Fe_2Al_5 alloy layer *vs*. total hot-dipping time.

Considering the service requirements of the coating: the thickness was about 100μm, too thick to produce cracks, too thin can not play a protective role, in addition to consider the uniformity of the coating and its industrial production costs, the 2min + 2min hot-dipping time coatings were more in line with the actual service requirements. Therefore, in the later study, we had chosen the 2min+2min hot-dipping time specimens for the study.

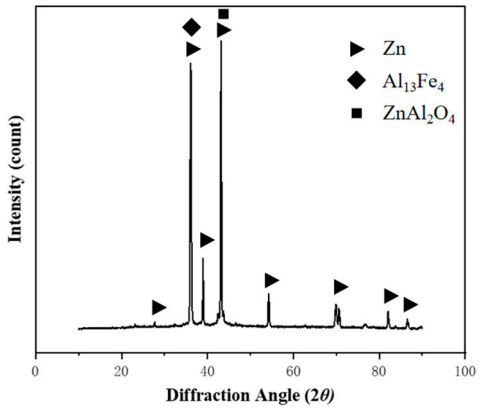

Figure 3. XRD patterns of 2min+2min hot-dipping time specimen's surface.

The XRD patterns (PDF #00-0110 for Zn, #50-0797 for $Al_{13}Fe_4$ & #71-0968 for $ZnAl_2O_4$) and phase diagrams of aluminum-zinc alloys [33] shown that the surface of the coatings consisted of Zn, $Al_{13}Fe_4$, and $ZnAl_2O_4$. Despite the second step of hot-dip galvanizing, Al and Fe elements still diffused to the surface, where Fe elements mainly combined with Al elements to form $Al_{13}Fe_4$.

Preprints (www.preprints.org) | NOT PEER-REVIEWED | Posted: 7 August 2023 doi:10.20944/preprints202308.0484.v1

In summary, the hot-dip galvanizing of Q345 steel after the hot-dip aluminizing of the steel surface avoided the occurrence of "silicon reactivity", in which the Fe element combines mainly with the Al element to form Fe-Al compounds.

3.2. Analysis of corrosion resistance of plated layer

3.2.1. Neutral salt spray test results

Figure 4 shown the macroscopic morphology of the surface of the sample with 2min+2min hot-dipping time after different time of neutral salt spray corrosion, it can be seen that with the growth of the corrosion time, the corrosion product accumulates on the surface of the sample, the color was slightly darkened, the brightness did not have any obvious change, and the surface was corroded to the unevenness, but the macroscopic cracks were not obvious.

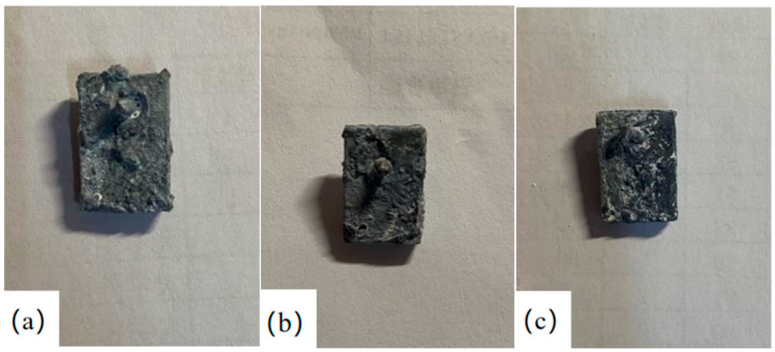

Figure 4. Macroscopic morphology of samples with 2min+2min hot-dipping time after different neutral salt spray corrosion time (a) 120h (b) 240h (c) 360h.

A review of the literature [34,35] yielded the kinetic equation for weight loss in neutral salt spray corrosion of Q345 steel as:

$$\Delta m = Kt^n \tag{3}$$

where, Δm is the weight loss of the sample (mg/cm^2), t is the total time of two-step hot-dipping (min), and K and n are constants.

Figure 5 shown the weight loss kinetic curve of neutral salt spray corrosion of the samples, which was fitted according to Eq. (3), and it can be concluded that the neutral salt spray corrosion weight loss kinetics of the substrate was given by Eq:

$$\Delta m' = 11.10437t^{0.99522} \tag{4}$$

Preprints (www.preprints.org) | NOT PEER-REVIEWED | Posted: 7 August 2023 doi:10.20944/preprints202308.0484.v1

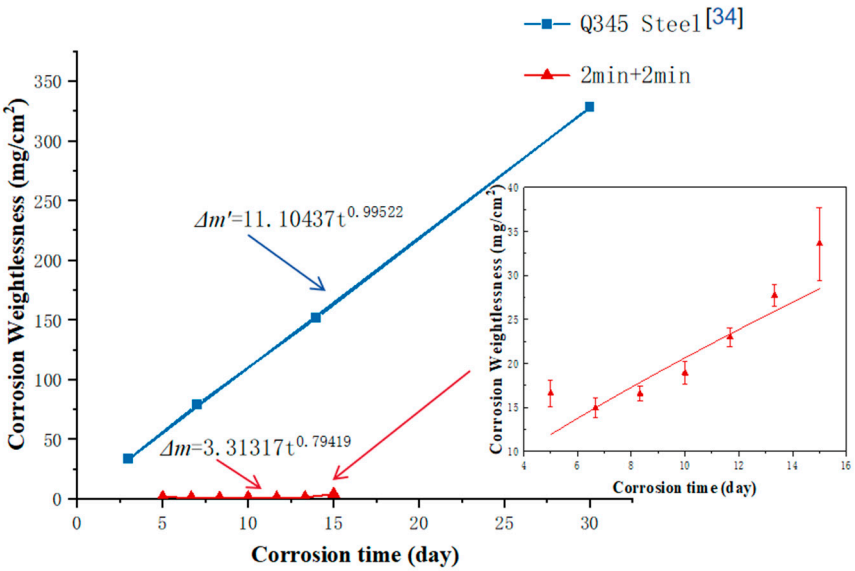

Figure 5. Variation of sample weight loss with corrosion time.

The kinetic equation for weight loss in neutral salt spray corrosion for Al-Zn composite coatings was:

$$\Delta m = 3.31317t^{0.79419} \quad (5)$$

It can be seen that the weight loss of Al-Zn composite coatings basically increases with time. However, the lowest corrosion rate was observed at 240 h, indicating the optimum corrosion performance, while the corrosion resistance of the coating became worse at 360 h. The reason may be that, due to the prolonged corrosion, there was an excessive buildup of corrosion products on the surface of the samples, which had an effect on their corrosion rate. The weight loss curve was analyzed by comparing the weight loss curve of the substrate with that of the two-step hot-dipping, and it was obvious that the weight loss of the substrate was much larger than that of the coated sample by (4)/(5) = $3.35158t^{1.25312}$. Therefore, the two-step hot-dipping method can provide better corrosion resistance.

According to Figure 6, after 360h salt spray corrosion, the surface of the hot-dipping layer produces many small particulate materials, which were examined by EDS (Table 2) and XRD (Figure 7, $Zn_5(OH)_6(CO_3)_2$ was examined using PDF#99-0062, Zn was examined using PDF#04-0831, and Fe_2O_3 was examined using PDF#85-0599 vs. $Al_3Fe_5O_{12}$ was examined using PDF# 49-1657) were examined and found to be oxides of Zn as their major element. The corrosion of the two-step dipping Al-Zn layers produced two different patterns of chemical reactions: clustered and dense, multilayered. It was shown that cluster corrosion produces compounds with the largest proportions of Zn and O, and a relatively large amount of C, probably $Zn_5(OH)_6(CO_3)_2$. Upon analysis, it was found that dense, multilayered network corrosion produces elements such as Zn and O as well as Al. However, ZnO and Fe_2O_3 had a loose structure and were easily detached, which made their antirust effect become not strong enough to cause the corrosion of Al-Zn coatings. From Figure 8 as well as Table 3, it can be seen from the cross-section that the coating was still dominated by Fe_2Al_5, which had excellent chemical stability, denseness and excellent corrosion resistance stability, which can effectively prevent the penetration of corrosive substances, thus making the Al-Zn coating of the two-step hot-dipping have stronger corrosion resistance. In contrast, the film of $Zn_5(OH)_6(CO_3)_2$ was more compact, but its corrosion resistance was also relatively weak. We found that when the dip-coating time of the two-step hot-dipping Al-Zn composite coatings was extended, the content of $Zn_5(OH)_6(CO_3)_2$ decreases significantly, and in some cases, it was even eliminated completely (consistent with the results of the XRD analysis), whereas the content of elements such as Zn and O as well as Al increases significantly, which leads to a more compact corrosion product structure. It

Preprints (www.preprints.org) | NOT PEER-REVIEWED | Posted: 7 August 2023 doi:10.20944/preprints202308.0484.v1

can be shown that the silicon reactivity was suppressed and good corrosion resistance was achieved. Meanwhile, from the EDS surface scanning results of the cross-section in Figure 9, it can be further illustrated that a small amount of Si elements will diffused into the outermost Zn-rich layer, and the corrosive elements of O, Cl, and Na were mainly distributed in the outermost Zn-rich layer, and the Al-Zn composite coating can effectively play the role of corrosion prevention.

Table 2. EDS data (at.%) for the spot-scan in Figure 6.

Spectrum	O	Al	Cl	Fe	Zn
Spectrum1	70.75	0	0	0	29.25
Spectrum2	73.33	0	0	0	26.67
Spectrum3	10.46	1.79	1.14	1.04	85.57
Spectrum4	66.60	0	0	0	32.40
Spectrum5	67.35	0	0	0	32.65

Table 3. EDS data (at.%) for the spot-scan in Figure 8.

Spectrum	O	Na	Al	Cl	Fe	Zn
Spectrum1	16.70	0	2.43	1.18	1.65	78.04
Spectrum2	1.67	0	62.16	0	26.12	10.06
Spectrum3	0	0	63.35	0	27.68	8.97
Spectrum4	5.24	2.30	0	0	92.46	0

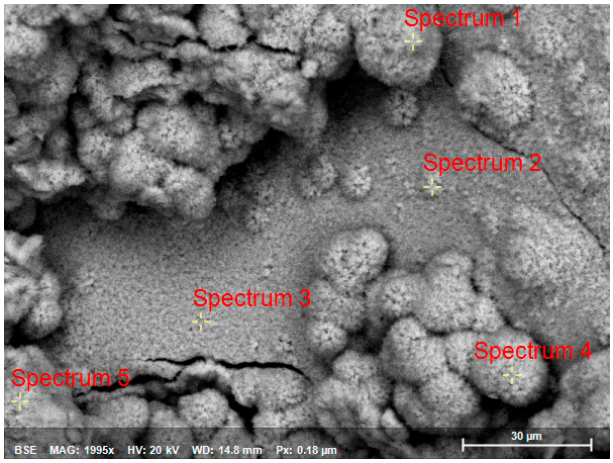

Figure 6. Microstructure of 2min+2min hot-dipping time coating's surface after 360h salt spray corrosion.

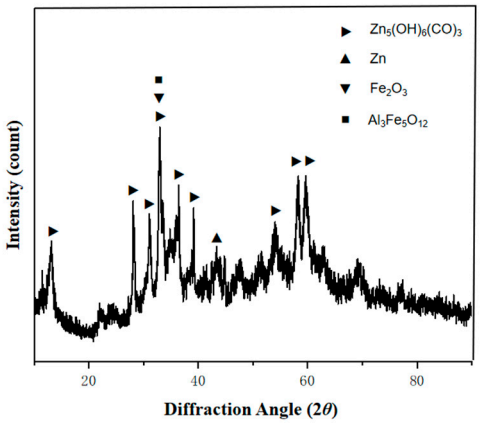

Preprints (www.preprints.org) | NOT PEER-REVIEWED | Posted: 7 August 2023 doi:10.20944/preprints202308.0484.v1

Figure 7. XRD patterns of 2min+2min hot-dipping time specimen's surface after 360h salt spray corrosion.

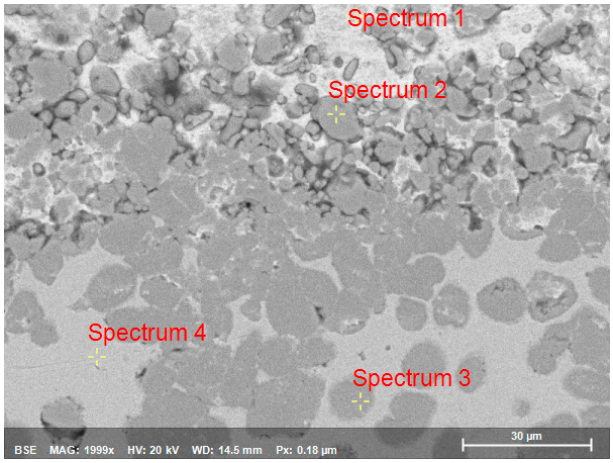

Figure 8. Microstructure of 2min+2min hot-dipping time coating's cross section after 360h salt spray corrosion.

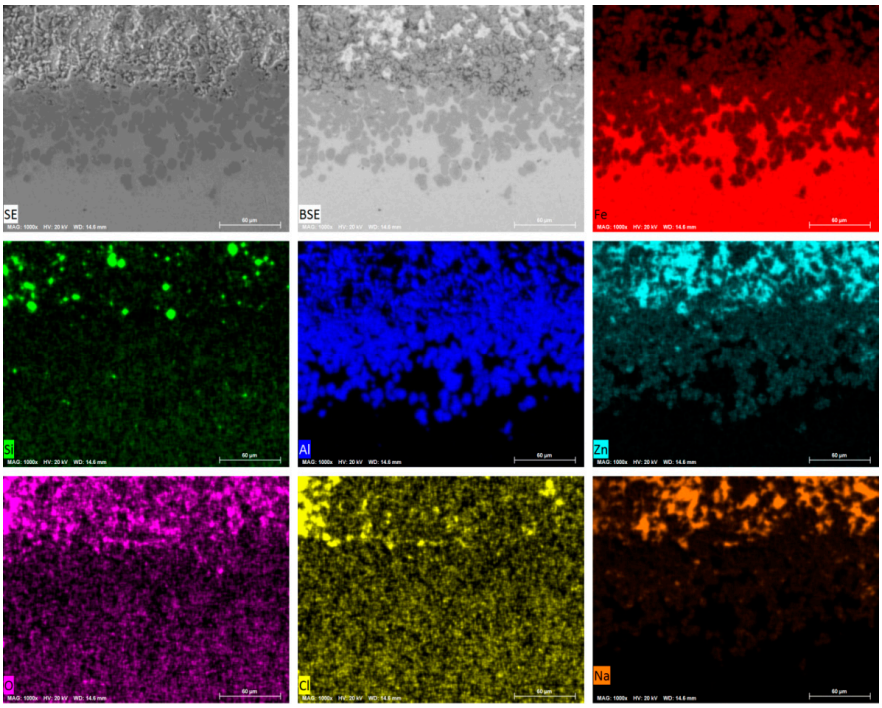

Figure 9. EDS mapping of 2min+2min hot-dipping time specimen's cross section after 360h salt spray corrosion.

3.2.2. Tafel polarization curves

According to the literature [36,37], we obtained the curve shown in Figure 10 by fitting the Tafel polarization curve, from which we can derive the corrosion potential of the hot-dipping Al-Zn composite coatings, which had an average value roughly in the vicinity of -0.92 V, which was close to two times smaller than the negative potential of the steel substrate, which confirms that the plated layer can provide a cathodic protection to the substrate [38]. The polarization curves of the hot-dipping Al-Zn composite coatings showed a similar pattern to that of the substrate, implying that the electrochemical reaction mechanism between them was almost identical. However, upon contact with the anode, its overlaying hot-dipping Al-Zn composite coatings produces a pronounced

Preprints (www.preprints.org) | NOT PEER-REVIEWED | Posted: 7 August 2023 doi:10.20944/preprints202308.0484.v1

passivation zone, which most likely originates from the production of a film of Al_2O_3-nH_2O oxides on its surface. The dense overlaying layer of Al_2O_3-nH_2O oxides effectively prevents corrosive species from penetrating into the hot-dipping Al-Zn composite coatings, which in turn enhances the corrosion resistance of the two-step hot-dipping Al-Zn composite coatings and gives it enhanced corrosion-resistant characteristics [39]. This was the main reason for the superior corrosion resistance of hot-dipping Al-Zn composite coatings. As shown in Table 4, the corrosion current of the two-step hot-dipping Al-Zn composite coatings was less than that of the substrate, which also indicates the superior corrosion resistance.

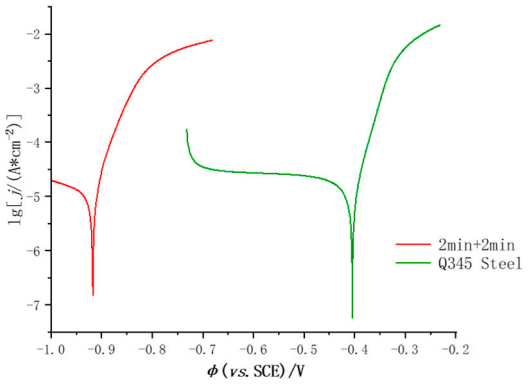

Figure 10. Polarization curves of 2min+2min hot-dipping time specimen and substrate in 3.5% NaCl solution.

Table 4. Polarization curve fitting results.

Specimen	φcorr(*vs.* SCE)/ V	*Lg*[*j*corr / (μA·cm^{-2})]
2min+2min	-0.917	-6.812
Q345 Steel	-0.405	-7.240

4. Conclusion

In this paper, the microstructure of two-step hot-dipping Al-Zn composite coatings on Q345 steel and the corrosion resistance of the coatings were studied, and the conclusions are as follows:

(1) The two-step hot-dipping coating consisted of Fe_2Al_5 and Al-Zn phases, and with the growth of hot-dipping time, the alloy layer was gradually densified, which can inhibit the "silicon reactivity" of Q345 steel.

(2) The thickness of the alloy phase layer of the hot-dipping Al-Zn composite coatings became thicker with the increase of the hot-dipping time, but the growth rate of the thickness slows down after the total hot-dipping time of 8 min.

(3) When the samples were corroded by neutral salt spray, $Zn_5(OH)_6(CO_3)_2$ appeared on the surface of the samples, and the corrosive elements of O, Cl, and Na were mainly distributed in the outermost Zn-rich layer, and the hot-dipping Al-Zn composite coatings showed strong corrosion resistance.

Author Contributions: Investigation, Data curation, and Writing – original draft, C.T.; Project administration, Methodology, and Writing – reviewed, F.L.. All authors have read and agreed to the published version of the manuscript.

Funding: This research was funded by the Science and Technology Project of Education Department of Hunan Province (No. 22A0100), Hunan Provincial Natural Science Foundation of China (No. 2021JJ30672).

Institutional Review Board Statement: Not applicable.

Informed Consent Statement: Not applicable.

Data Availability Statement: Not applicable.

Acknowledgments: The authors gratefully acknowledge the support provided by Materials Intelligent Design College Students' Innovation and Entrepreneurship Education Center, Xiangtan University, Xiangtan, Hunan, China.

Conflicts of Interest: The authors declare no conflict of interest.

References

1. Zhanshuo Liang, Weiyong Wang, Ziqi Wang,Effect of cold-form and tensile strain rate on mechanical properties of Q345 steel at elevated temperatures,Journal of Constructional Steel Research,Volume 191,2022,107192,ISSN 0143-974X,https://doi.org/10.1016/j.jcsr.**2022**.107192.
2. Marder A R. The metallurgy of zinc-coated steel [J]. Progress in materials science, **2000**, 45(3): 191-271
3. WANG S M, ZHAO X J, DANG J W, et al. Research status of the process mechanism of batch hot-dip galvanizing [J]. Surface Technology, **2016**, 45 (5): 19-25.
4. SHIH H C, HSU J W, SUN C N, et al. The lifetime assessment of hot-dip 5% Al–Zn coatings in chloride environments [J]. Surface and Coatings Technology, **2002**, 150 (1): 70-75.
5. R. Sa-nguanmoo, E. Nisaratanaporn, Y. Boonyongmaneerat, Corros. Sci. 53 (**2011**) 122.
6. LIU X, LIU C L, YU W G, et al. Effects of alloying elements on the platability and corrosion resistance of a new Zn–Mg–Ni–V–Al alloy coating [J]. Corrosion & Protection, **2018**, 39 (12): 924-929, 940.
7. FENG G, HOU J, ZHANG L. Effects of steel composition and adding elements on microstructure and properties of hot-dip galvanizing [J]. Hot Working Technology, **2011**, 40 (4): 118-121.
8. Sandlin R W. Galvanizing characteristics of different types of steel [J]. Wire and Wire Products, **1941**, 16: 28-35
9. A. Mertens, E.M. Bellhouse, J.R. McDermid,Microstructure and mechanical properties of a mixed Si–Al TRIP-assisted steel subjected to continuous galvanizing heat treatments,Materials Science and Engineering: A,Volume 608,**2014**,Pages 249-257,ISSN 0921-5093.
10. Ryabov, V.R. Aluminizing of Steel (Translated from the Russian Work: Alitirovanie Stali); Amerind Publishing Co. Pvt. Ltd.: New Delhi, India, **1985**.
11. Bahadur, A.; Mohanti, O.N. Structural studies of hot dip aluminized coatings on mild steel. Mater. Trans. JIM **1991**, 32, 1053–1061.
12. Heumann, T.; Dittrich, N.A. Structure character of the Fe2Al5 intermetallics compound in hot dip aluminizing process. Z Met. **1959**, 50, 617–623.
13. Eggeler, G.; Auer, W.; Kaesche, H. On the influence of silicon on the growth of the alloy layer during hot dip aluminizing. J. Mater. Sci. **1986**, 21, 3348–3350.
14. Lainer, D.I.; Kurakin, A.K. Mechanism of the effect of silicon in aluminum on the process of reactive diffusion of iron into aluminum. Fiz. Metal. Metalloved. **1964**, 18, 145.
15. Zarei, F.; Nuranian, H.; Shirvani, K. Effect of Si addition on the microstructure and oxidation behaviour of formed aluminide coating on HH309 steel by cast-aluminizing. Surf. Coat. Technol. **2020**, 394, 125901.
16. Wang, C.J.; Chen, S.M. The high-temperature oxidation behavior of hot-dipping Al–Si coating on low carbon steel. Surf. Coat. Technol. **2006**, 200, 6601–6605.
17. Huang, X.; Xiao, K.; Fang, X.; Xiong, Z.; Wei, L.; Zhu, P.; Li, X. Oxidation behavior of 316L austenitic stainless steel in high temperature air with long-term exposure. Mater. Res. Express **2020,** 7, 066517.
18. Abro, M.A.; Hahn, J.; Lee, D.B. High temperature oxidation of hot-dip aluminized T92 steels. Met. Mater. Int. 2018, 24, 507–515.
19. Zhang, G.; Yang, F.; Lu, G.; Xiang, X.; Tang, T.; Wang, X. Fabrication of Al 2 O 3/FeAl coating as tritium permeation barrier on tritium operating component on quasi-CFETR scale. J. Fusion Energy **2018**, 37, 317–324.
20. Chen, J.; Li, X.; Hua, P.; Wang, C.; Chen, K.; Wu, Y.; Zhou, W. Growth of inter-metallic compound layers on CLAM steel by HDA and preparation of permeation barrier by oxidation. Fusion Eng. Des. **2017**, 125, 57–63.
21. Cheng, W.J.; Wang, C.J. Study of microstructure and phase evolution of hot-dipped aluminide mild steel during high-temperature diffusion using electron backscatter diffraction. Appl. Surf. Sci. **2011**, 257, 4663–4668.

22. Badaruddin, M. Improvement of high temperature oxidation of low carbon steel exposed to ethanol combustion product at 700 ℃ by hot-dip aluminizing coating. Makara J. Technol. **2012**, 15, 137–141.
23. Yan Lei, Cheng Shumao. Technology analysis of Steel wire hot-dip galvanized aluminum alloy [J]. Wire and Cable, **2018** (4): 17-19, 31.
24. TACHIBANA K, MORINAGA Y, MAYUZUMI M. Hot dip fine Zn and Zn-Al alloy double coating for corrosion resistance at coastal area [J]. Corrosion Science, **2006**, 49 (1): 149-157.
25. Xiong Ziliu, ZHANG Yunfei, Jiang Tao. Properties, characteristics and development status of Zn-Al alloy coating [J]. Hebei Metallurgy, **2012** (4): 8-11, 24.
26. Lu Jintang, Jiang Aihua, Che Chunshan, et al. Research progress of hot dipping Zn-Al alloy coatings [J]. Material Protection, **2008**, 41 (7): 47-51, 88.
27. YAN L, CHENG S M. The introduction of hot dipped zinc–aluminum alloy technology for steel wire [J]. Electric Wire & Cable, **2018** (4): 17-19, 31.
28. PENG H P, SU X P, WANG J H, et al. Interface reaction mechanism for galvanizing in Zn–Al baths [J]. The Chinese Journal of Nonferrous Metals, **2012**, 22 (11): 3168-3175.
29. WANG Q Y, ZHANG L, LU J Y, et al. Microstructure and corrosion resistance of zinc–aluminum alloy coating prepared by a two-step hot dipping process [J]. Electroplating & Finishing, **2020**, 39 (7): 392-398.
30. QIAO H, LI Z, YANG J, et al. Effect of Si content on microstructure and corrosion resistance of hot-dip Zn–Al alloy coating [J]. Heat Treatment of Metals, **2018**, 43 (8): 178-183.
31. ZHANG Y Y, ZHANG Y L, LI Q, et al. Influencing mechanism of alloy elements on structure and performance of Zn–Al hot dip coating [J]. The Chinese Journal of Process Engineering, **2009**, 9 (Suppl.1): 465-472.
32. Marder, A.R. The metallurgy of zinc-coated steel. Prog. Mater. Sci. **2000**, 45, 191–271.
33. Han W. Effect of Si on the growth kinetics of Fe2Al5 phase during Fe-Al reaction [D]. Xiangtan University,**2009**.
34. Zhang Qiang, Dai Fu Hua, Si Yi et al. Microstructure and salt spray Corrosion Behavior of surfacing Joint of Q345C Steel for bogies [J]. Electric Welding Machine,**2016**,46(06):107-111.
35. Liu Wei, Li Honglin, Wu Haixu, et al. Corrosion behavior of 6061-T4 aluminum alloy in salt spray environment [J]. Materials protection, 2022, zhongguo kuangye daxue (11) : 37-43. DOI: 10.16577 / j.i SSN. 1001-1560.**2022**.0305.
36. LAN Y J. Electrochemical corrosion behavior of Q235 steel in sodium chloride contaminated silt [D]. Taiyuan university of technology, 2022. DOI: 10.27352 /, dc nki. Gylgu. **2022**.001846.
37. Wang Zhen, Jin Libing, Liang Xinya. Effect of surface state on electrochemical corrosion behavior of Q235 steel in solutions with different chloride ion concentrations [J]. Electroplating and Finishing, **2019**,42(04):6-12.DOI:10.19289/j.1004-227x.**2023**.04.002.
38. YUAN M, LUO X Y, YAO Z J. Influence of addition of Mg, RE(La, Ce) on corrosion resistance of hot dipping 55% Al-Zn -- 1.6%Si coating [J].Journal of Nanjing University of Aeronautics & Astronautics, **2015**, 47 (5):696-701.
39. Tan Chengyu, WEI Xiuyu, Chen Zhun. Study on corrosion resistance of Zn-5%Al-RE coating [J]. Electroplating and Environmental Protection, **2002**, 22 (5): 29-32.